

NANO EXPRESS

Open Access



Heating-up Synthesis of MoS₂ Nanosheets and Their Electrical Bistability Performance

Xu Li^{1,2}, Aiwei Tang^{1*}, Jiantao Li¹, Li Guan², Guoyi Dong² and Feng Teng^{1,2*}

Abstract

Molybdenum disulfide (MoS₂) nanosheets were synthesized by using a simple heating-up approach, in which 1-dodecanethiol (DDT) was used not only as a sulfur source but also as the surface ligand. The sheet-like morphology was confirmed by the transmission electron microscopy (TEM) and atomic force microscopy (AFM) results, and the X-ray diffraction (XRD) patterns and Raman spectrum were employed to characterize the structure of the as-synthesized MoS₂ nanosheets. The as-obtained MoS₂ nanosheets blending with a polymer could be used to fabricate an electrically bistable device through a simple spin-coating method, and the device exhibited an obvious electrical bistability in the *I-V* curve. The charge transport of the device was discussed based on the organic electronic models.

Keywords: MoS₂, Nanosheets, Electrically bistable device, Charge transport

Background

In the past few decades, much attention has been paid to the two-dimensional (2D) nanomaterials due to their surprising unique physical, electrical, and chemical properties arising from high surface area and quantum confinement effects in two dimensions [1–3]. Therefore, the 2D nanomaterials exhibit wide potential applications in various applications, such as optoelectronic devices, energy conversion, and bio-sensing [4–9]. To date, different types of 2D compounds have been developed, and layered transition metal dichalcogenides (TMDCs) have become one of the most popular objectives due to their indirect-to-direct bandgap transition when exfoliated to monolayer and possessing intriguing optical properties [4, 9]. Therefore, it is necessary to exploit synthetic strategies to prepare TMDC nanocrystals. Till now, different synthetic approaches including chemical vapor deposition [10, 11], ion-intercalation and exfoliation [12, 13], and colloidal chemical synthesis [14, 15] have been developed for synthesis of TMDCs. Among these different synthetic methods, colloidal chemical synthesis is widely used in the preparation of ultrathin 2D nanomaterials. Although some progress has been made in the colloidal

synthesis of 2D nanomaterials, some challenges still remain in this field. Therefore, it is interesting to develop a simple heating-up (non-injection) method to prepare molybdenum disulfide (MoS₂) nanosheets, which is reliable and does not need any injection and pre-synthesis of precursors.

In this paper, a simple heating-up colloidal chemical approach has been developed to prepare MoS₂ nanosheets, which involves the direct heating of the mixture of molybdenum precursors and 1-dodecanethiol (DDT) in the non-coordinating solvent. The crystal structure, morphology, and chemical composition of the as-obtained products were characterized by X-ray diffraction (XRD) patterns, Raman spectra, transmission electron microscopy (TEM), atomic force microscopy (AFM), and X-ray photoelectron spectroscopic (XPS) techniques. The MoS₂ nanosheets could disperse well in the semiconducting polymer, which was used to fabricate sandwiched structured electrically bistable devices. An obvious electrical bistability was observed in the current-voltage (*I-V*) results, and the charge transport mechanism was discussed based on the organic electronic models.

Methods

A typical synthesis MoS₂ nanosheets is described as follows. Stoichiometric of Mo(acac)₂, DDT, and 1-octadecene

* Correspondence: awtang@bjtu.edu.cn; fteng@bjtu.edu.cn

¹Key Laboratory of Luminescence and Optical Information, Ministry of Education, School of Science, Beijing Jiao Tong University, Beijing 100044, China

Full list of author information is available at the end of the article

(ODE) were mixed in a 50-ml three-necked flask, and then the reaction solution was purged through nitrogen for 20 min under magnetic stirring. Afterwards, the mixture was heated to 280 °C slowly under the protection of nitrogen and kept at the temperature for 4 h. After the completion of the reaction, the reaction mixture was cooled down to room temperature naturally after removal of the heating source. The MoS₂ nanosheets were obtained by addition of excess ethanol and centrifuged at 6000 rpm for 10 min, and then the precipitates were redispersed in chloroform. The precipitation and washing process was repeated twice, and the as-obtained products were dispersed in chloroform or dried in vacuum for next characterization.

The as-obtained MoS₂ nanosheets were mixed with poly (N-vinylcarbazole) (PVK) in chlorobenzene, in which the weight ratio of MoS₂ to PVK was 1:1 and the total concentration was 20 mg/mL. The electrically bistable device was fabricated as follows: the glass substrate coated with an indium-tin-oxide (ITO) anode was pre-cleaned and then the poly (3, 4-ethylenedioxy-thiophene):poly-(styrene-sulfonate) (PEDOT:PSS) was spin-coated onto the substrate as a buffer layer and then annealed at 150 °C for 15 min. Afterwards, the MoS₂:PVK thin film was formed by using a spin-coating technique. Finally, the Al top electrodes were thermally evaporated through a shadow mask at a pressure of approximately 10⁻⁶ Torr.

The XRD patterns were measured by a D8 ADVANCE X-ray diffractometer. The thermogravimetric analysis (TGA) and differential thermal gravity (DTG) were taken on a PYRISI thermal gravimetric analyzer. The Raman spectrum was obtained using HR Evolution Raman spectrometer. TEM images were collected by Tecnai G2 F20 transmission electron microscope. The AFM patterns of MoS₂ nanosheets were measured in Bruker Multimode 8 Scanning probe microscopes (SPMs). The XPS measurements were performed on an ESCALAB 250 spectrometer with a 300-W Al K α radiation source. The *I-V* characteristics of the devices were measured by using a Keithley Source Meter 2612 controlled by a computer. All the measurements were carried out at room temperature.

Results and Discussion

To gain the decomposition information of the Mo-thiolate precursors, Fig. 1 depicts the TGA and DTG results of the precursors. As shown in the TGA curve, a rapid weight loss is observed in the elevating temperature from 150 to 350 °C, in which two steps appear at about 230 and 320 °C, respectively. Accordingly, the DTG curve displays two obvious peaks at 236 and 331 °C. Based on the previous report [16], the weight loss between 150 to 280 °C arises from the volatilization or decomposing of DDT and

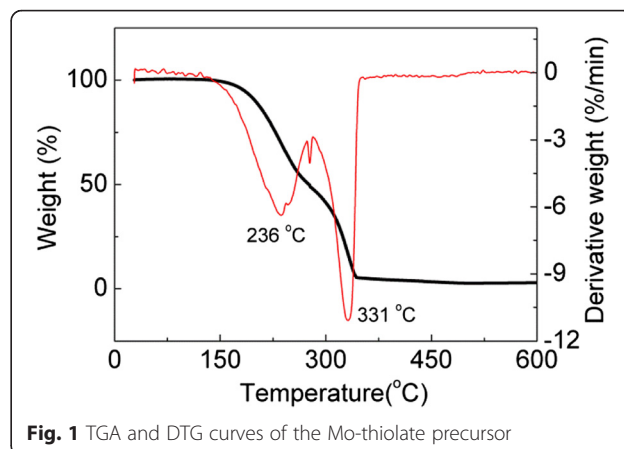


Fig. 1 TGA and DTG curves of the Mo-thiolate precursor

the other decomposition region from 280 to 350 °C may be attributed to the decomposing of ODE.

The chemical composition and valence state of MoS₂ nanosheets were studied by XPS spectra. Figure 2 depicts the high-resolution XPS results of Mo 3d and S 2p. As shown in Fig. 2a, two peaks located at 232.6 and 229.4 eV are observed, which can be ascribed to Mo 3d_{3/2} and Mo 3d_{5/2} of 2H-phase MoS₂, respectively. The binding energy positions of the two peaks confirm the valence of Mo is +4, which is consistent with the previous report [17]. As can be seen in Fig. 2b, the S 2p peak can be fitted by using a spin-orbit separation of 1.1 eV, and the doublet peaks are located at 162.3 (S 2p_{3/2}) and 163.4 eV (S 2p_{1/2}), which are the characteristic of sulfide of the Mo–S bond [18]. The atomic ratio of S to Mo is estimated to be 2.6:1 based on the XPS results, which is higher than the stoichiometric ratio of MoS₂, which may arise from the capping ligand of DDT.

To further confirm the DDT coating on the surface of MoS₂ nanosheets, the Fourier transform infrared spectroscopy (FTIR) of MoS₂ nanosheets is given in Fig. 3. Two obvious sharp peaks at 2914 and 2846 cm⁻¹ correspond to the asymmetric methyl stretching (CH₃) and asymmetric methylene (CH₂) stretching modes, respectively [19]. The FTIR peak at 1462 cm⁻¹ belongs to the scissoring of –CH₂–, and the two peaks at 773 and 730 cm⁻¹ are the characteristic peaks of CH₃ rocking origin [20]. As compared to the free DDT, the band at 2577 cm⁻¹ disappears in the MoS₂ nanosheets, which indicates the formation of Mo–S bond [21]. All the FTIR information confirms the DDT capping on the surface of the nanosheets.

The crystal structure of the as-obtained MoS₂ nanosheets has been confirmed by the XRD patterns shown in Fig. 4a, the diffraction peaks are broadened due to the nature of their very small size. All the diffraction peaks can match well with the bulk hexagonal MoS₂ (JCPDS No. 24-0513). The Raman spectrum was used to further analyze the molecular structure, which is shown in

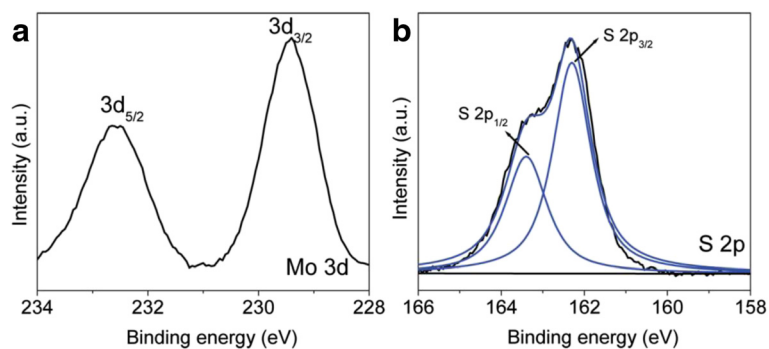


Fig. 2 High-resolution XPS results of **a** Mo 3d and **b** S 2p of MoS₂ nanosheets

Fig. 4b. Two strong bands are located at 379.3 and 404.8 cm⁻¹, which are ascribed to the in-plane vibrational (E_{2g}¹) and the out-of-plane vibrational (A_{1g}) modes, respectively [22, 23]. This is in good agreement with the previous report, which demonstrates the formation of MoS₂.

The morphology of MoS₂ nanosheets obtained at different reaction times were characterized by the TEM images, and the TEM images are shown in Fig. 5. As shown in Fig. 5a, b, d, the as-obtained products are like nanowires at first glance; however, all the products exhibit a sheet-like morphology after careful observation, which can be confirmed by the edge of the products shown in Fig. 5d. As a matter of fact, the flexural fold is present in the product due to their ultrathin thickness of the nanosheets. The typical HRTEM image of the product obtained at 120 min shown in Fig. 5c indicates their good single crystallinity. To further confirm the morphology of nanosheets, the AFM images of the products obtained at 240 min were measured, and a typical AFM image as well as the as topographic height profile are

presented in Fig. 6. The AFM images depicted in Fig. 6a indicate that the size of the nanosheet is up to hundreds of nanometers, and the height of the selected two parts is measured to be 2–3 nm, which is equivalent to 4–5 monolayer thickness for S–Mo–S structures [24].

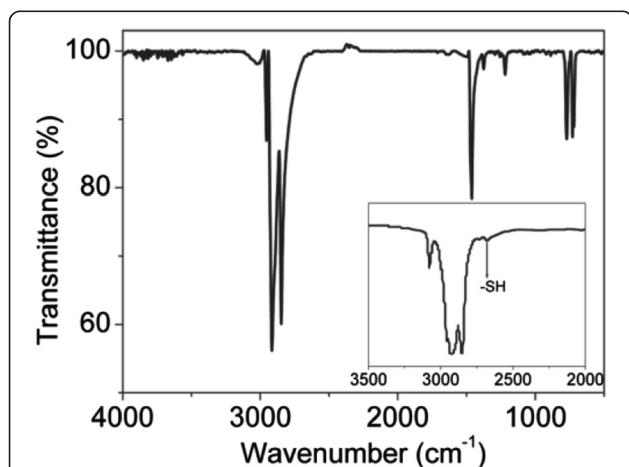


Fig. 3 FTIR spectrum of DDT-capped MoS₂ nanosheets. The *inset* shows the FTIR spectrum of free DDT

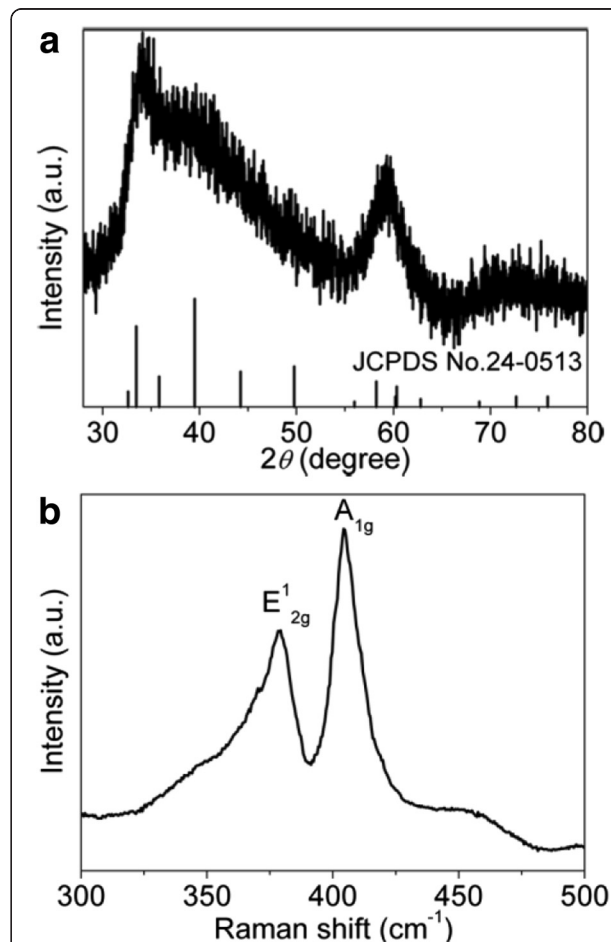


Fig. 4 **a** XRD patterns and **b** Raman spectrum of MoS₂ nanosheets

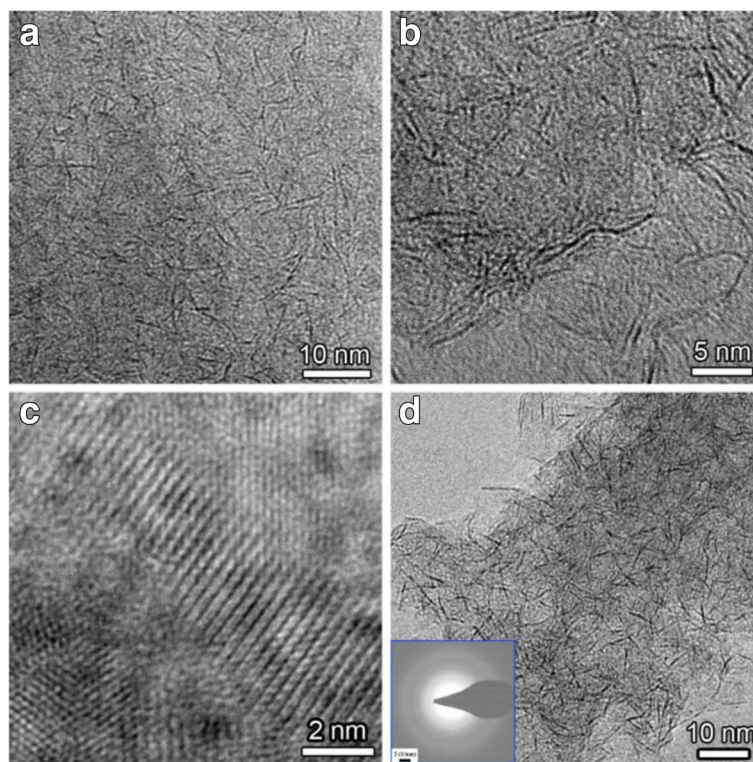


Fig. 5 TEM images of MoS₂ nanosheets obtained at different reaction times: **a** 30 min, **b** 120 min; **d** 240 min, and **c** the HRTEM image of MoS₂ nanosheets obtained at 120 min

Electrical bistability of the metal sulfide nanocrystals was reported in previous literatures, which often displayed two different conducting states at the same sweeping voltage [25–27]. However, the electrical bistability of the MoS₂ nanosheets was rarely reported. Herein, a sandwiched electrically bistable device was fabricated based on the blending film composed of MoS₂ nanosheets and PVK by using a simple spin-coating method, in which the MoS₂ nanosheets were dispersed in PVK matrix to make the film more smooth. The schematic illustration of the device fabrication process and the device structure is given in Fig. 7a, b. As shown in Fig. 7c, an obvious electrical hysteresis is observed when the sweeping voltage is scanned from –3 V to 3 V and then from 3 to –3 V, which exhibits a high-conducting state (ON state) and a low-conducting state (OFF state) at the same sweeping voltage. Such an electrical hysteresis behavior is an essential feature for the electrically bistable device. As the sweeping voltage is scanned from 0 to 3 V, the current is increased rapidly when the sweeping voltage exceeds about 2 V, which indicates that the conducting state transforms from an OFF to ON state. When the sweeping voltage scans from 0 to –3 V, the current reaches its maximum at about –1.5 V, and then decreases quickly with the reverse voltage increasing, which is a typical negative differential resistance (NDR) behavior. As a result, the

conducting state changes from an ON to OFF state. As stated in our previous report [27], the electrical bistability is not observed in the device based on only the PVK film, which indicates that the MoS₂ nanosheets play a significant role in the electrical bistability.

In order to understand the switching and the charge transport mechanism of the electrically bistable device based on MoS₂ nanosheets and PVK, Fig. 8 shows the experimental and fitting data of the I - V curves in the region of positive voltage. Generally, the carrier transport mechanism of the electrically bistable device can be described by space charge-limited current (SCLC) and trap-controlled space charge-limited current (TCLC) [25], thermionic emission (TE) [26], and ohmic conduction model [27]. As shown in Fig. 8a, the $\log I$ is in proportion to $V^{1/2}$ in the region from 0 to 1.5 V of the OFF state, which matches well with the TE model. However, when the voltage increases from 1.5 to 2 V for the OFF state, the relationship between $\log I$ and $\log V$ can be fitted by a line with a slope of 13.2, which is attributed to the TCLC conduction model in this region (Fig. 8b). When the conduction state transits from an OFF to ON state, the experimental data ($\log I$ versus $\log V$) in the sweeping voltage region of 0–3 V can be fitted by a straight line with a slope of 1.43, which is close to the ohmic model (Fig. 8c).

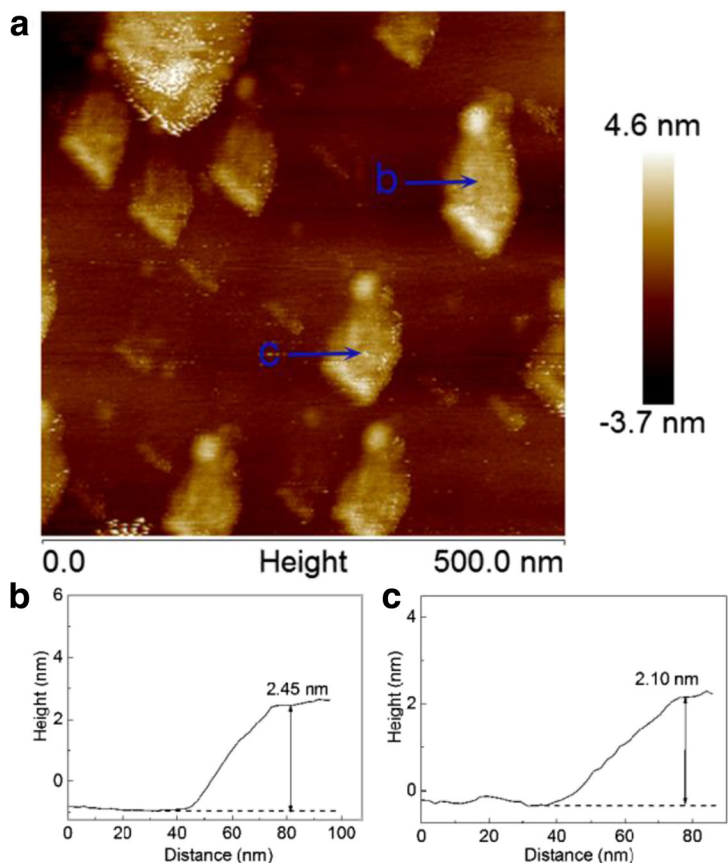


Fig. 6 a A typical AFM image of MoS₂ nanosheets obtained at 240 min and **b, c** the topographic height profiles of the two parts labeled in **a**

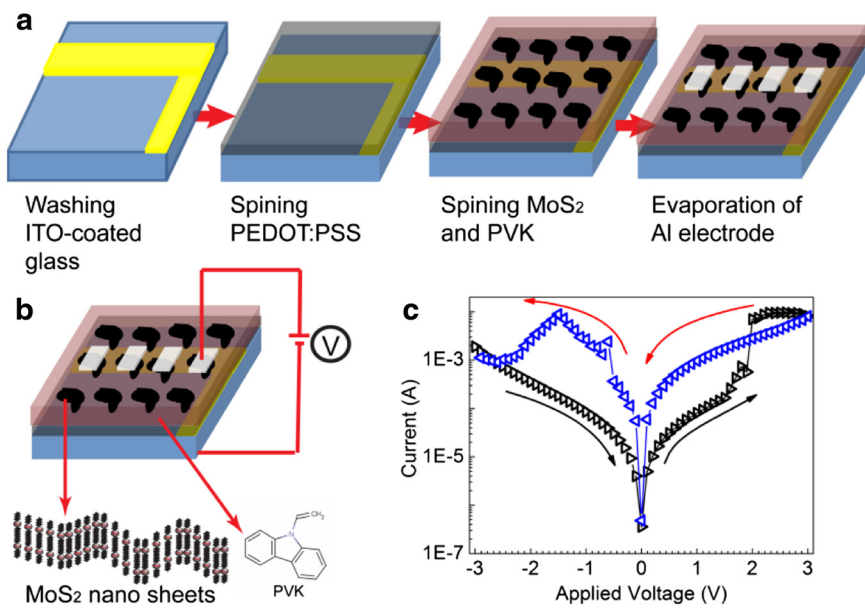
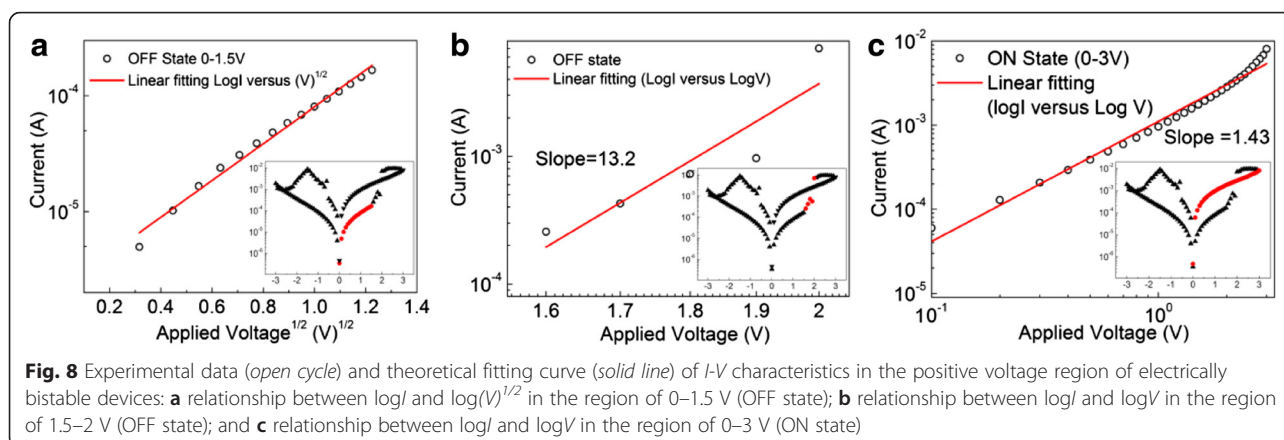


Fig. 7 a Schematic illustration of the fabrication process of the electrically bistable devices, **b** device structure and the molecular structure of PVK, and **c** current-voltage of the device



Conclusions

In summary, a simple heating-up colloidal approach was developed to prepare MoS₂ nanosheets, which was synthesized in DDT and non-coordinating solvent. The as-obtained products had a sheet-like morphology, whose crystal structure was characterized by the XRD patterns and Raman spectrum. An electrically bistable device was fabricated based on the blends of MoS₂ nanosheets and PVK, and an obvious electrical bistability and NDR behavior was observed in the *I-V* curves. The charge transport could be described in terms of the organic electronic models, and the charge transport mechanism changed from the thermionic emission to the ohmic model during the transition of the conducting state from an OFF state to ON state. The result indicates that the MoS₂ nanosheets may have potential application in the organic/inorganic hybrid electrically bistable devices.

Competing interests

The authors declare that they have no competing interests.

Authors' contributions

XL and LG synthesized the MoS₂ nanosheets and measured the properties of the nanosheets. JL and AT prepared the electrically bistable devices and carried out the electrical measurement. GD and FT conceived and designed the study. XL and AT wrote the manuscripts. All authors read and approved the final manuscript.

Acknowledgements

This work is partly supported by the Fundamental Research Funds for the Central Universities (2014JBZ010) and the National Nature Science Foundation of China (No. 61125505, No.61205180). The authors (XL, LG) also appreciate the financial support from the Midwest Universities Comprehensive Strength Promotion Project.

Author details

¹Key Laboratory of Luminescence and Optical Information, Ministry of Education, School of Science, Beijing Jiao Tong University, Beijing 100044, China. ²Hebei Key Laboratory of Optic-electronic Information and Materials, College of Physics Science and Technology, Hebei University, Baoding 071002, People's Republic of China.

Received: 12 February 2016 Accepted: 21 March 2016

Published online: 31 March 2016

References

- Chhowalla M, Shin HS, Eda G, Li LJ, Loh KP, Zhang H (2013) The chemistry of two-dimensional layered transition metal dichalcogenide nanosheets. *Nat Chem* 5:263
- Babaei H, Khodadadi JM, Sinha S (2014) Large theoretical thermoelectric power factor of suspended single-layer MoS₂. *Appl Phys Lett* 105:193901
- Li LL, Wu GH, Yang GH, Peng J, Zhao JW, Zhu JJ (2013) Focusing on luminescent graphene quantum dots: current status and future perspectives. *Nanoscale* 5:4015–4039
- Morozov YV, Kuno M (2015) Optical constants and dynamic conductivities of single layer MoS₂, MoSe₂, and WSe₂. *Appl Phys Lett* 107:083103
- Das S, Demarteau M, Roelofs A (2015) Nb-doped single crystalline MoS₂ field effect transistor. *Appl Phys Lett* 106:173506
- Perkins FK, Friedman AL, Cobas E, Campbell PM, Jernigan GG, Jonker BT (2013) Chemical vapor sensing with monolayer MoS₂. *Nano Lett* 13(2):668–673
- Baek SH, Choi Y, Choi W (2015) Large-area growth of uniform single-layer MoS₂ thin films by chemical vapor deposition. *Nanoscale Res Lett* 10:388
- Khazaeinezhad R, Kassani SH, Nazari T, Jeong H, Kim JK, Choi K, Lee JU, Kim JH, Cheong H, Yeom DI, Oh K (2015) Saturable optical absorption in MoS₂ nano-sheet optically deposited on the optical fiber facet. *Opt Com* 335:224
- Ye J, Li XL, Zhao JJ, Mei XL, Li Q (2015) A facile way to fabricate high-performance solution-processed n-MoS₂/p-MoS₂ bilayer photodetectors. *Nanoscale Res Lett* 10:454
- Lee YH, Zhang XQ, Zhang WJ, Chang MT, Lin CT, Chang KD, Yu YC, Wang JTW, Chang CS, Li LJ, Lin TW (2012) Synthesis of large-area MoS₂ atomic layers with chemical vapor deposition. *Adv Mater* 24:2320–2325
- Song L, Ci LJ, Lu H, Sorokin PB, Jin CH, Ni J, Kвашnin AG, Kвашnin DG, Lou J, Yakobson BI, Ajayan PM (2010) Large scale growth and characterization of atomic hexagonal boron nitride layers. *Nano Lett* 10:3209–3215
- Zeng ZY, Sun T, Zhu JX, Huang X, Yin ZY, Lu G, Fan ZX, Yan QY, Hng HH, Zhang HY et al (2012) An effective method for the fabrication of few-layer-thick inorganic nanosheets. *Angew Chem Int Ed* 51:9052–9056
- Zhang J, Zhang H, Dong SH, Liu YP, Nai CT, Shin HS, Jeong HY, Liu B, Loh KP (2014) High yield exfoliation of two-dimensional chalcogenides using sodium naphthalenide. *Nat Commun* 5:2995
- Yoo D, Kim M, Jeong S, Han J, Cheon J (2014) Chemical synthetic strategy for single layer transition metal chalcogenides. *J Am Chem Soc* 136:14670–14673
- Son JS, Yu JH, Kwon SG, Lee J, Joo J, Hyeon T (2011) Colloidal synthesis of ultrathin two-dimensional semiconductor nanocrystals. *Adv Mater* 23:3214–3219
- Tang AW, Qu SQ, Li K, Hou YB, Teng F, Cao J, Wang YS, Wang ZG (2010) One-pot synthesis and self-assembly of colloidal copper(I) sulfide nanocrystals. *Nanotechnology* 21:285602
- Yin ZY, Zhang X, Cai YQ, Chen JZ, Wong JI, Tay YY, Chai JW, Wu J, Zeng ZY, Zheng B, Yang HY, Zhang H (2014) Preparation of MoS₂-MoO₃ hybrid nanomaterials for light-emitting diodes. *Angew Chem Int Ed* 53:12560
- Eda G, Yamaguchi H, Voiry D, Fujita T, Chen MW, Chhowalla M (2011) Photoluminescence from chemically exfoliated MoS₂. *Nano Lett* 11:5111
- Snyder RG, Strauss HL, Elliger CA (1982) Carbon-hydrogen stretching modes and the structure of n-alkyl chains. 1. Long, disordered chains. *J Phys Chem* 86:5145
- Porter MD, Bright TB, Allara DL, Chidsey CED (1987) Spontaneously organized molecular assemblies. 4. Structural characterization of n-alkyl thiol

- monolayers on gold by optical ellipsometry, infrared spectroscopy, and electrochemistry. *J Am Chem Soc* 109:3559
21. Sandhyarani N, Pradeep T (2001) An investigation of the structure and properties of layered copper thiolates. *J Mater Chem* 11:1294
 22. Huang JW, Dong ZP, Li YR, Li J, Tang WJ, Yang HD, Wang J, Bao Y, Jin J, Li R (2013) MoS₂ nanosheet functionalized with Cu nanoparticles and its application for glucose detection. *Mater Res Bull* 48:4544–4547
 23. Feng QL, Duan KY, Ye XL, Lu DB, Du YL, Wang CM (2014) A novel way for detection of eugenol via poly (diallyldimethylammonium chloride) functionalized graphene-MoS₂ nano-flower fabricated electrochemical sensor. *Sensor Actuat B* 192:1–8
 24. Zhao J, Zhang ZC, Yang SS, Zheng HL, Li YB (2013) Facile synthesis of MoS₂ nanosheet-silver nanoparticles composite for surface enhanced Raman scattering and electrochemical activity. *J Alloy Comp* 559:87–91
 25. Ham JH, Oh DH, Cho SH, Jung JH, Kim TW (2009) Carrier transport mechanisms of nonvolatile write-once-read-many-times memory devices with InP–ZnS core-shell nanoparticles embedded in a polymethyl methacrylate layer. *Appl Phys Lett* 94:112101
 26. Tang AW, Teng F, Hou YB, Wang YS, Tan FR (2010) Optical properties and electrical bistability of CdS nanoparticles synthesized in dodecanethiol. *Appl Phys Lett* 96:163112
 27. Li JT, Tang AW, Li X, Cao YP, Wang M, Ning Y, Lv LF, Lu QP, Lu YZ, Hu YF, Hou YB, Teng F (2014) Negative differential resistance and carrier transport of electrically bistable devices based on poly (N-vinylcarbazole)-silver sulfide composites. *Nano Res Lett* 9:128

Submit your manuscript to a SpringerOpen[®] journal and benefit from:

- Convenient online submission
- Rigorous peer review
- Immediate publication on acceptance
- Open access: articles freely available online
- High visibility within the field
- Retaining the copyright to your article

Submit your next manuscript at ► springeropen.com
